

THE REVIEW OF SCIENTIFIC INSTRUMENTS

VOLUME 42, NUMBER 8

AUGUST 1971

Analysis of Heat Exchangers for Dilution Refrigerators

J. D. SIEGWARTH AND RAY RADEBAUGH

Cryogenics Division, NBS Institute for Basic Standards, Boulder, Colorado, 80302

(Received 16 February 1971)

Numerical calculations of the behavior of dilution refrigerator heat exchangers are discussed and some results for both discrete and continuous exchangers are presented. It is shown that thermal conductance along the stream is negligible for a typical continuous exchanger of the coaxial tube type, but becomes a dominant feature of a typical discrete exchanger operating below about 50 mK and degrades the performance considerably. A simple design change can be made that reduces the conductance along the liquid and improves the performance of such an exchanger. A simple means of determining whether conductivity is important in either continuous or discrete exchangers is given.

INTRODUCTION

CONSTRUCTION details for counterflow heat exchangers used in continuously operating dilution refrigerators have been discussed by several authors.¹⁻⁸ The main design considerations are⁷ that the liquid volume be as small as possible so equilibrium can be established rapidly when the temperature is changed, the impedance to the flowing liquids be small, the thermal conductivity of the exchanger between the two streams be adequate, and the heat transfer areas be as large as possible to overcome the effects of the Kapitza resistivity. The lowest temperature achievable in the mixing chamber depends upon the effectiveness of these heat exchangers.

Some analyses of these exchangers have been done in the past,^{3,5,9,10} but various simplifying approximations, such as zero or infinite liquid thermal conductivities, were made so that the differential equations governing heat transfer could be solved analytically. However, to analyze some types of exchangers and, in any case, to include proper conductivities and heat capacities, the differential equations must be solved numerically. To predict or optimize exchanger performance, proper conductivities, heat capacities, etc., must be used.

Two types of counterflow exchangers are commonly used in dilution refrigerators. The discrete type, first used by Wheatley *et al.*,³ consists of blocks containing two cavities (see Fig. 1) into which a high surface area material is sintered. High conductivity copper is generally used for both the filler and the body. The exchanger usually consists

of four to six of these blocks connected together with short lengths of low conductivity tubing such that the incoming stream passes through one cavity and the exit stream passes through the other cavity of each block. The other type is the continuous exchanger, in which there are no discontinuous changes in physical parameters over the full

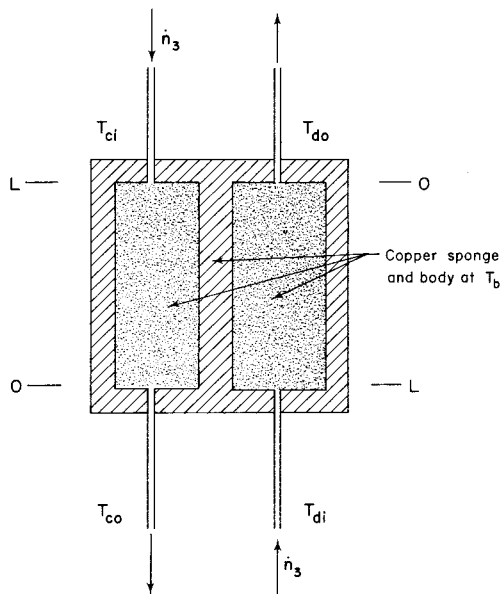


FIG. 1. Schematic of a copper block exchanger showing lengths L , flow directions \hat{n}_s , and temperatures. The temperatures T_{ci} , T_{co} , T_{di} , and T_{do} are those of the concentrated inlet and outlet and dilute inlet and outlet streams, respectively.

length of the exchanger. An example of this type is the coaxial tube exchanger first used in dilution refrigerators by Ehnholm *et al.*,⁴ which consists of a long, small diameter Cu-Ni tube loosely fitted inside a larger Cu-Ni tube. The incoming stream passes through the central tube while the return stream passes through the annulus. This particular type is gaining popularity because it is simple to construct and has a small liquid volume. In this paper, more detailed analyses of the discrete and continuous exchangers are presented.

I. GENERAL CONSIDERATIONS

The two coupled differential equations describing both types of heat exchangers can be derived from the heat balance on a fluid control volume of length dx . The steady state flow equation, for the fluid on each side, is

$$A_j \left[\underbrace{\kappa_j \frac{d^2 T_j}{dx^2}}_{\text{heat conduction}} + \frac{d\kappa_j}{dx} \left(\frac{dT_j}{dx} \right)^2 \right] - \underbrace{\frac{d\sigma_j}{dx}}_{\text{Kapitza conduction}} \int_{T_b}^{T_i} \frac{dT}{\rho_j} + \underbrace{W_j - \dot{n}_3 C_j}_{\text{viscous heating}} = \underbrace{\frac{dT_j}{dx}}_{\text{enthalpy change}}, \quad (1)$$

where j is a general label that will be replaced with c when the concentrated stream is considered, or by d when the dilute stream is considered. The Joule-Thomson cooling of ^3He in the dilute stream due to an osmotic pressure drop across the exchanger is negligible¹⁰ compared with the viscous heating that would occur simultaneously. Using the appropriate boundary conditions, this set of equations is solved numerically with a digital computer to determine the temperature profiles of the concentrated and dilute streams, $T_c(x)$ and $T_d(x)$, respectively. A library subroutine¹¹ employing the Runge-Kutta method is used in the program. The various parameters are x , the position in the exchanger along the direction of flow; A_j , the liquid cross sectional area perpendicular to the direction of flow; κ_j , the liquid thermal conductivity; $d\sigma_j/dx$, the heat transfer surface area per unit length of exchanger; ρ_j , Kapitza resistivity; T_b , the temperature of the heat exchanger body; \dot{n}_3 , ^3He molar flow rate; and, C_j , the molar specific heat of the liquid stream. The viscous heating of the moving liquids, W_j , may cause some heating at the lowest temperatures³ but will be considered negligible here.

Since mixer temperatures of 0.01 K or higher are being considered here, thermal relaxation effects between ^3He quasiparticles and phonons in the dilute solution are considered small and not included.³ Analytic expressions are used for ρ_j , κ_j , and C_j in the solution of Eq. (1).

The expression for Kapitza resistivity,

$$\rho_c = [(20 \times 10^{-5})/T_c^3] (\text{cm}^2 \cdot \text{K}/\mu\text{W}), \quad (2a)$$

was determined from the data of Anderson *et al.*,¹² and is

valid between 0.01 and 0.13 K. In most cases discussed here, it is assumed that this dependence continues to 0.7 K. In some cases, which will be discussed further below, the equation,

$$\rho_c = \left(\frac{2.4}{T_c^4} + \frac{1.55}{T_c^3} \right) \times 10^{-5} \left(\frac{\text{cm}^2 \cdot \text{K}}{\mu\text{W}} \right), \quad (2b)$$

is used from $0.13 < T_c < 0.7$ K. This expression more correctly fits the data of Anderson *et al.*,¹² in this temperature range.

The boundary resistance between a nearly saturated dilute solution and copper has been measured by Wheatley *et al.*³ up to 0.1 K. There is some deviation from a T^{-3} dependence, but for this work it is assumed that

$$\rho_d = [(7 \times 10^{-5})/T_d^3] (\text{cm}^2 \cdot \text{K}/\mu\text{W}) \quad (3)$$

up to 0.2 K. Since there are presently no data on the commonly used 70/30 Cu-Ni alloys, Eqs. (2a), (2b), and (3) are used for the boundary impedance of this material also.

For the liquid thermal conductivity, κ_j , the results of Abel *et al.*^{13,14} were fitted by

$$\kappa_c = \left(\frac{3.48}{T_c} + 31.4 + 58.1 T_c \right) \left(\frac{\mu\text{W}}{\text{cm} \cdot \text{K}} \right). \quad (4)$$

An expression for the dilute side conductivity has been determined for the case of constant ^4He chemical potential, μ_4 , by interpolating the data of Abel *et al.* to the appropriate concentrations. A significant correction¹³ is applied for the small pore size which occurs in a sintered copper exchanger. The expressions determined for this conductivity are

$$\begin{aligned} \kappa_d &= 5.4 \times 10^3 (T_d - 0.045) \left(\frac{\mu\text{W}}{\text{cm} \cdot \text{K}} \right); & T_d > 0.1 \text{ K} \\ \kappa_d &= 3 \times 10^5 \left(T_d^3 + \frac{2.6}{T_d} \right) \left(\frac{\mu\text{W}}{\text{cm} \cdot \text{K}} \right); & T_d < 0.1 \text{ K}. \end{aligned} \quad (5)$$

The expression for the heat capacity of the concentrated ^3He , C_c , was taken from calculations by Radebaugh.¹⁵ The term C_d is C_{μ_4} , the heat capacity at constant osmotic pressure¹⁵ which is weakly dependent on the mixer temperature T_m . For all calculations presented here, T_m is small enough that the error is small if T_m is assumed to be zero. The dilute stream flow impedance must be small also since C_{μ} is an equilibrium value under zero flow conditions, i.e., no pressure drop in the dilute stream. Preliminary measurements¹⁶ of C_{μ_4} indicate agreement to better than 10% between the calculated and experimental results for T less than 0.2 K. Analytic expressions for C_d have been determined by polynomial fitting of the calculated values of C_{μ_4} for $T_m = 0$. The analytic expressions used for C_{μ_4} and tables of the liquid enthalpies are given in the Appendix.

II. DISCRETE EXCHANGERS

A. Method of Calculation

The calculation is simplified considerably if it is assumed the copper body is at constant temperature. This assumption is generally made. An unpublished report on some experimental work by Ehnholm and Wheatley indicates that this assumption is reasonable for the heat fluxes encountered in these heat exchangers. Equation (1) is solved for each side of the exchanger (see Fig. 1) subject to the condition that the net heat transferred to the heat exchanger body is zero.

The optimum volume ratio of the two sides of a discrete exchanger is obtained by specifying some volume, V_3 , of pure ^3He liquid that is to be divided between the two sides of the exchanger in such a way that the heat transferred is a maximum. The liquid cross sectional areas of the heat exchanger are expressed in terms of V_3 and f , the fraction of the ^3He contained in the dilute side. These areas are

$$A_c = (1-f)V_3/L \quad (6a)$$

for the concentrated side, assuming only pure ^3He present, and

$$A_d = (fV_3/L)[27.58/X_\mu + 7.6 + 1.65X_\mu^2]/36.83 \quad (6b)$$

for the dilute side. The exchanger length is L and the expression in brackets is the volume of dilute solution in cubic centimeters per mole of ^3He , where X_μ is the ^3He concentration, and 36.83 cm^3 is the molar volume of pure ^3He .¹⁵ The optimum value of f is found by maximizing the heat transferred in the exchanger. The ratio of dilute side to concentrated side volume can be calculated from f and the molar volumes.

The condition on the thermal gradient at the exchanger tube interface is

$$A(dT_j/dx)_{\text{tube}} = A_j(dT_j/dx)_{\text{exchanger}}, \quad (7)$$

where A is the tube cross section. The interconnecting tubes between exchangers and the connecting tubes to the still and mixer are sufficiently small so that the heat conducted through them can be neglected. Thus, at the exit end of the heat exchanger cavity, $dT_j/dx=0$ by Eq. (7) for both concentrated and dilute streams because the dT_j/dx in the tube at this end must be zero when there is no conductance between exchangers. Within the inlet tubes, the temperature of the concentrated or of the dilute stream can be higher or lower, respectively, than the liquid in the exchanger. Conductance of the liquid in the tube changes the temperature of the stream just before it enters the exchanger. The slopes at the inlet end are not known and starting the problem at this end requires an iteration to arrive at the exit end with $dT_j/dx=0$. This iteration is avoided by starting the calculation at the exit end.

The dilute side behavior is calculated first; hence $j=d$ in Eq. (1). Values for T_b and T_{do} , where T_{do} is the dilute

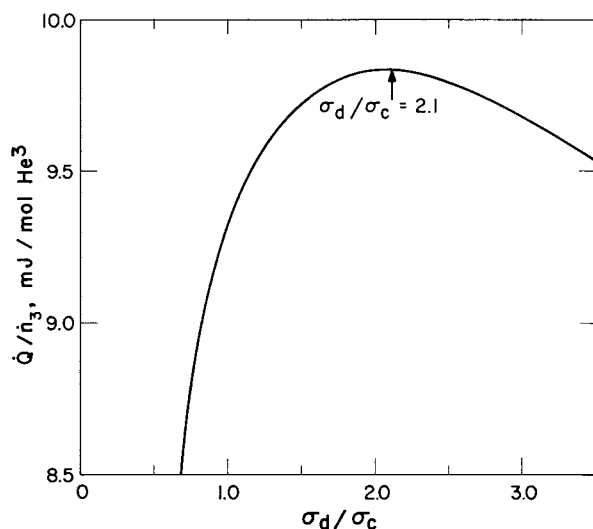


FIG. 2. Total heat transfer rate \dot{Q} in the discrete exchanger with $\sigma_v = 400 \text{ cm}^{-1}$ as a function of the ratio of dilute to concentrated surface areas, σ_d/σ_c , for a fixed number of moles of ^3He in the exchanger. The quantity \dot{n}_3 is the ^3He circulation rate.

side outlet temperature (see Fig. 1), are assumed and the calculation is carried from $x=0$ to L . Since it is desired that the mixer temperature T_m be fixed, the calculation for the lowest heat exchanger is iterated with respect to T_b until the change in enthalpy of the incoming stream prior to entering the exchanger is equal to the heat transferred out of the exchanger via liquid conduction to the incoming stream. That is, the equation,

$$H_d(T_{dL}) - H_d(T_{di}) = \kappa_d \frac{A_d}{\dot{n}_3} \left(\frac{dT_d}{dx} \right)_{x=L}, \quad (8)$$

is satisfied. The term $H_d(T)$ is the dilute stream enthalpy, T_{dL} is the temperature of the liquid in the input end of the heat exchanger, and $T_{di} = T_m$. For each choice of T_{do} , a unique value for T_b is calculated.

If it is assumed that the concentrated stream is 100% ^3He and there is no heat input to the mixer, then, from an enthalpy balance on the mixer,¹⁵

$$T_{co} = T_{di}/0.36, \quad (9)$$

where T_{co} is the concentrated side output temperature. The concentrated side behavior is calculated using Eq. (1) with $j=c$ and Eq. (9). The final value of T_b from the dilute side calculation is the T_b used for the concentrated side calculation. The enthalpy changes on the two sides generally will not be equal, so a second iteration is done varying T_{do} until these changes are equal. For each change in T_{do} the dilute side must be recalculated as described above to find the new value of T_b . The value of T_{ci} is chosen such that the enthalpy changes of the concentrated and dilute streams are equal.

The next exchanger up the line can now be calculated using the T_{do} calculated above as the new T_{di} , using the

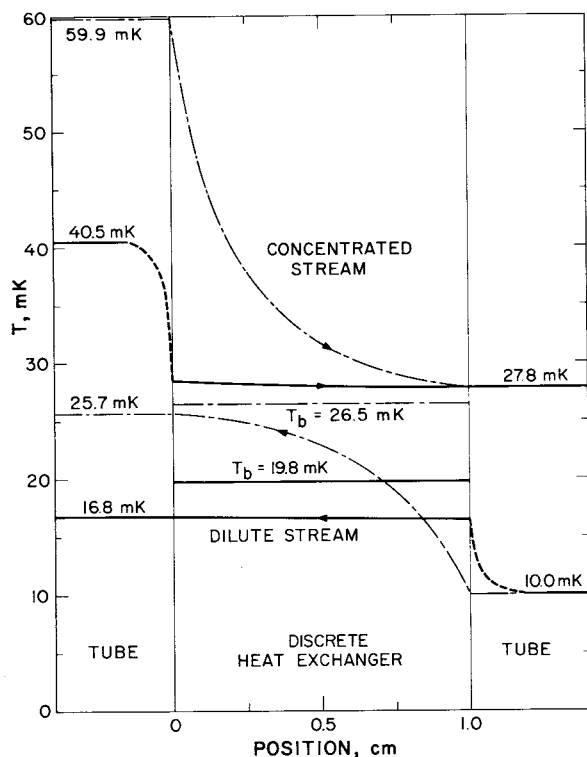


FIG. 3. Calculated liquid and body temperature profiles within and near the discrete exchanger for both zero and finite liquid conductivity, κ_j . The ratio σ_d/σ_c is the optimum, 2.1, $\sigma_v = 400 \text{ cm}^{-1}$, and $\dot{n}_3 = 2 \times 10^{-5}$ moles/sec. --- $\kappa_j = 0$; — $\kappa_j \neq 0$.

T_{ci} above as the new T_{co} , and using an estimated value for T_b . The iterative process outlined above is repeated.

B. Results and Discussion

The results presented here are all for heat exchangers 10.0 mm long with a V_3 of 1 cm^3 except when otherwise noted. These quantities are similar to those used in actual practice. Results are shown for two examples with different surface areas but the same values for σ_c/\dot{n}_3 . In the first example, the surface area per cubic centimeter of liquid, given by

$$\sigma_v = \sigma_j / LA_j,$$

is $400 \text{ cm}^2/\text{cm}^3$ in both sides and the flow rate is 2×10^{-5} moles/sec. In the second case, $\sigma_v = 6000 \text{ cm}^{-1}$ and the flow

rate is 3×10^{-4} moles/sec. The first example has a flow rate and surface area closer to typical values, although the surface area is given a value smaller than actual areas as there is some evidence¹⁷ to suggest the effective areas may be smaller than the actual areas.

By solving the problem for various values of the fraction f in Eq. (6), and plotting f vs the heat transferred between streams, the optimum ratio of volumes on the two sides of the exchanger can be found. Figure 2 is a plot of the heat transferred as a function of σ_d/σ_c , the ratio of surface areas for the lowest temperature with $\sigma_v = 400 \text{ cm}^{-1}$ and flow rate of 2×10^{-5} moles/sec. The ratio σ_d/σ_c is equivalent to the ratio of volumes when the same sponge particle size and density are used on each side. The optimum ratio occurs at $\sigma_d/\sigma_c = 2.1$ ($f = 0.15$) for the lowest temperature heat exchanger, but the sensitivity of the transferred heat to this ratio is low. For $T_{co} \cong 0.1 \text{ K}$ the maximum occurs at the same value of f , but σ_d/σ_c is now 2.5 due to the decrease of ^3He concentration in the dilute solution. The heat transfer at a T_{co} of 0.1 K is less sensitive to σ_d/σ_c than is shown by the curve of Fig. 2, for which T_{co} is about 0.028 K.

In Fig. 3, the behavior of the lowest temperature exchanger with $T_m = 10 \text{ mK}$ is shown, where $\sigma_v = 400 \text{ cm}^{-1}$ and $\sigma_d/\sigma_c = 2.1$, ($f = 0.15$). Curves for T_c , T_d , and T_b are shown as a function of x through the body, with an extrapolation of T_c and T_d into the outside tubes shown also. The incoming stream temperature profiles immediately outside the exchanger are estimated using the slopes determined from Eq. (7), along with T_{di} and T_{ci} , which are equivalent to the outlet temperatures of the adjacent exchangers. The conductivities of the liquids are so high that ΔT_d is less than 0.4 mK and ΔT_c less than 0.7 mK inside the exchanger. Most of the temperature change occurs in the interconnecting tube just prior to entering the heat exchanger for this case. The ΔT_j of the liquids in the exchanger are small compared to $|T_j - T_b|$. This is true when the conductance through the liquid is very large compared to the conductance to the walls, i.e.,

$$A_j \kappa_j \rho_j / L \sigma_j \gg 1. \quad (10)$$

The heat exchanger performance is relatively independent of κ_j when Eq. (10) is true. For the exchanger with the

TABLE I. Calculated inlet and outlet temperatures and effectiveness R of the model exchanger. The first four lines of the table are data for a series of interconnected exchangers operating between 0.67 and 0.01 K. The last three lines are modifications of the lowest temperature exchanger. The temperatures T_{ci} , T_{co} , T_{di} , and T_{do} are those of the concentrated stream inlet and outlet and the dilute stream inlet and outlet, respectively.

Exchanger	Total vol of ^3He	T_{ci}	T_{co}	T_{di}	T_{do}	R
No. 1	1 cm^3	40.5 mK	27.78 mK	10.0 mK	16.77 mK	36%
2	1	72.86	40.5	16.77	31.25	59
3	1	183.2	72.86	31.25	70.03	95
4	$\frac{1}{4}$	672.7	183.2	70.03	180.25	>99
1	2	48.8	27.78	10.0	20.73	58
1 (Composed of two)	2	72.86	27.78	10.0	31.25	123
1 (3 partitions)	1	51.66	27.78	10.0	22.06	65

smaller surface area, the left side of Eq. (10) is about 3.4 for the concentrated side. The liquids may be considered isothermal and, to avoid solving Eq. (1), a set of simultaneous algebraic equations can be used to roughly determine the exchanger behavior. In Fig. 4, the results are shown for the larger surface area exchanger. The left side of Eq. (10) is now approximately 0.2 for the concentrated side and ΔT_j is quite large. In this case the heat exchanger behavior can only be determined from solutions of Eq. (1).

The dotted curves in Fig. 3 show the behavior at the $\kappa_j=0$ limit for $T_m=10$ mK. Similar curves exist, but are not shown, for the $\sigma_v=6000$ cm⁻¹ exchanger, and give a T_{ci} of 0.0625 K. The heat transferred between the streams in the $\kappa_j=0$ limit is about three times as great as in the $\kappa_j \neq 0$ case. From this result it is apparent that the large liquid conductivity can considerably degrade the exchanger performance.

Table I shows the inlet and outlet temperatures of some heat exchangers. The relative effectiveness, listed in the last column, compares the performance of one of these exchangers with a discrete exchanger capable of producing the maximum possible change of T_c , but with the same T_{co} . This relative effectiveness, R , is defined by

$$R = \{(T_{ci} - T_{co}) / [(T_{ci})_{\text{perfect}} - T_{co}]\}. \quad (11)$$

The temperature T_{co} rather than T_{ci} is held fixed in this definition¹⁸ of R since the calculations must be done with a

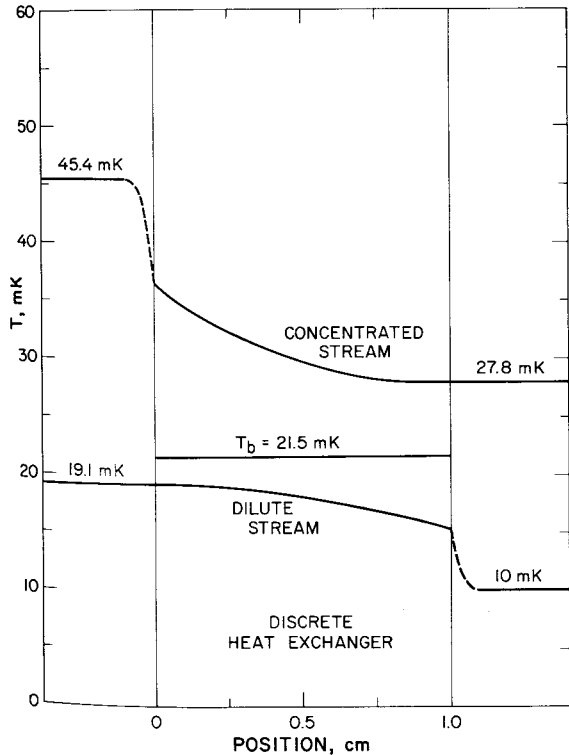


FIG. 4. Calculated liquid and body temperature profiles for the same discrete exchanger shown in Fig. 3, but with $\sigma_v=6000$ cm⁻¹ and $\dot{n}_3=3 \times 10^{-4}$ moles/sec. $\kappa_i \neq 0$.

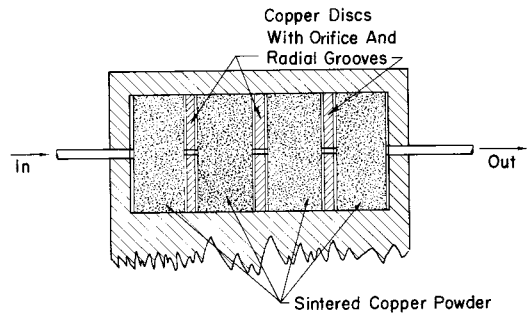


FIG. 5. One half of a discrete exchanger with partitions for reducing liquid conductance. The radial grooves prevent a high flow impedance.

set T_{co} . The perfect discrete heat exchanger has an infinite surface area; thus, $T_{co}=T_{do}$.

The first four lines of Table I show the results of calculations of successive heat exchangers from a mixer temperature of 10 mK up to a still temperature of 0.67 K for the dimensions and flow rate described above. Five exchangers of the type described above with $\sigma_v=400$ cm² are required for a 0.7 K still temperature. A 1 cm³ volume of ³He for the highest temperature exchanger is so excessively large that T_b , T_{do} , and T_{co} are nearly equal and convergence difficulties were encountered in the iterative parts of the solution. The volume of ³He was reduced by a factor of 4 for this exchanger to aid convergence. In practice, five exchangers have been required.³

The relative effectiveness is high for the warmest exchanger shown in Table I, but decreases quite rapidly with decreasing T . The fifth line shows the change in R upon doubling the size ($V_3=2$ cm³) of the coldest exchanger, whereas the sixth line shows R for a system of two exchangers of $V_3=1$ cm³ each. The R given for this combination is relative to a single discrete exchanger. As would be expected, it is considerably more effective to add volume as additional exchangers rather than enlarging the existing exchangers.

It is apparent from Fig. 3 that the performance of a heat exchanger can be improved by reducing conductance through the liquid. Making the exchanger long and small in cross section can accomplish this, but the flow impedance would probably be too high. The effect of the liquid conductivity in the discrete heat exchanger can be reduced rather easily by inserting several tight fitting disks or partitions into the chamber, dividing the sintered material into sections as shown in Fig. 5. These disks would be about 1 mm thick and have one hole through them whose inside diameter is the same as or slightly smaller than that of the interconnecting tubing. These hole dimensions are such that the liquid thermal conductance between compartments is small and will be neglected for purposes of this calculation. Figure 6 shows the calculated temperatures as a function of x in the exchanger in which $\sigma_v=400$ cm⁻¹, but now with three disks inserted. This is compared to the

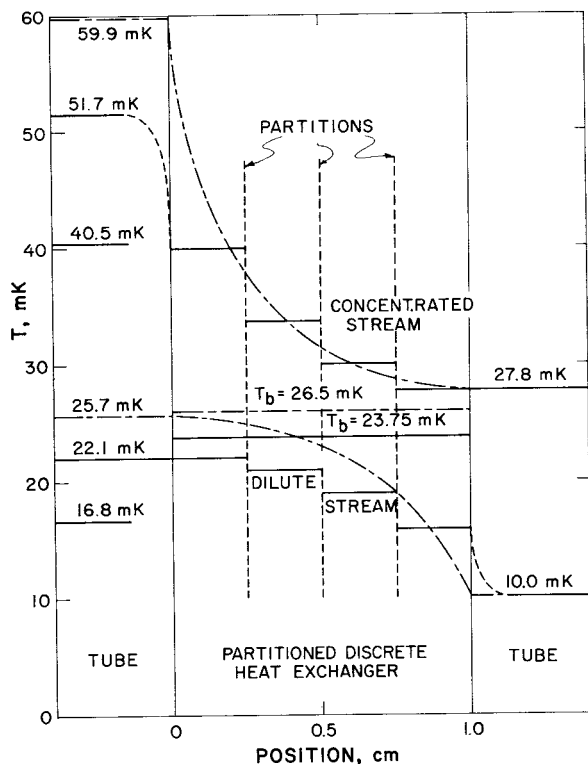


FIG. 6. The temperature profile of the exchanger of Fig. 3 with three partitions added. The values of T_{d0} and T_{ci} for the unpartitioned case are shown on the left side. The profiles for a liquid conductivity κ_j of 0 are shown for comparison. --- $\kappa_j = 0$; — $\kappa_j \neq 0$.

$\kappa_j = 0$ case shown also in Fig. 3. The heat transfer is over twice that of the undivided exchanger. The relative effectiveness, given in the last line of Table I, is nearly doubled by three dividers. An exchanger of this type can give the same performance as an unpartitioned exchanger of a much larger size. Thus all discrete exchangers should be made with the partitions unless they already behave nearly like the $\kappa_j = 0$ case. This modification can be made without adding any external joints to the dilution system, which avoids additional leak possibilities. Forming four sections would increase the exchanger length by only 3 mm for 1 mm thick disks.

Experimental data are presently not available on the various inlet, outlet, and body temperatures for the discrete exchangers, so no comparison can be made between experimental and calculated performance of one discrete exchanger; however, a comparison with experimental results for a set of heat exchangers is possible. The minimum number of exchangers required to achieve a T_m of 10 mK can vary between four and five for the exchangers calculated here, though five are required experimentally. Comparison of experimental and calculated results for individual exchangers would probably determine why the calculated results indicate fewer exchangers are needed. Additional work is in progress which will permit one to design a more optimum set of discrete exchangers to reach a desired mixer temperature.

III. CONTINUOUS EXCHANGER

A. Method of Calculation

Continuous exchangers will be divided into two categories: ideal and nonideal. The former has sufficiently small liquid and tube cross sections, such that the heat conducted parallel to the flow is negligible compared to the total heat transferred; i.e.,

$$\sum_j \frac{A_j \kappa_j}{L \dot{n}_3 C_j} \ll 1,$$

where L is the total length of the continuous exchanger. The index j is summed over c , d , and b which refer to the concentrated stream, dilute stream, and body, respectively. However, the heat capacity C_b should best be given a value equal to C_d . The inequality above can be written as

$$\sum_j \frac{B_j A_j}{L \dot{n}_3} \ll 1, \quad (12)$$

where $B_j = \kappa_j / C_j$. The term B_j is a weak function of temperature and can be approximated by

$$B_j \approx 4 \times 10^{-5} \text{ moles} \cdot \text{cm}^{-1} \cdot \text{sec}^{-1}$$

for both the dilute and concentrated liquids. For channel sizes the order of 50μ , B_d is reduced by a factor of only about 2 due to boundary effects on κ_d . For the ideal continuous exchanger, the conductivity terms in Eq. (1) are neglected.

A continuous exchanger for which Eq. (12) is not true is considered nonideal. The value of the term on the left side of Eq. (12) can serve as a crude approximation to the deviation from the behavior of the ideal continuous exchanger, provided the term is still somewhat smaller than 1. The exact behavior in the nonideal case can be found only by solving Eq. (1) with all terms included.

The behavior of an exchanger with no heat conduction along the tube walls is found when the differential Eqs. (1) for T_d and T_c are solved simultaneously. This solution is subject to the condition that the net heat to the intermediate wall is zero at all points along the exchanger. That is,

$$\frac{d\sigma_c}{dx} \int_{T_b}^{T_c} \frac{dT}{\rho_c} = \frac{d\sigma_d}{dx} \int_{T_d}^{T_b} \frac{dT}{\rho_d}. \quad (13)$$

This can be integrated analytically when ρ_j is given by Eqs. (2a) and (3) and the result can be solved for T_b . This integral can be done analytically when ρ_c is given by Eq. (2b), but the integrated equation must be solved for T_b by iteration.

The solution at the mixer end of the exchanger is subject to the condition

$$[H_d(T_d)]_{\text{solubility curve}} = \dot{Q} / \dot{n}_3 + H_c(T_{co}), \quad (14)$$

where the first term is the dilute solution enthalpy on the solubility curve, \dot{Q} is the heat into the mixer due to thermal leakage and experimental heat loads, and the last term is the enthalpy of the pure ^3He entering the mixer. Equation (14) is satisfied by iterating the problem with respect to T_{do} .

B. Results and Discussion

Particular emphasis is given in this work to the small diameter coaxial tube exchangers. Since the tube diameters used in coaxial heat exchangers are generally quite small, the exchanger can almost always be considered ideal. The left side of Eq. (12) is usually the order of 10^{-3} for both liquid streams and even less than 10^{-3} for both the tube walls. Since data are not available for the boundary resistance between the liquids and stainless steel or Cu-Ni tubing generally used in coaxial tube exchangers, it is assumed that the heat transfer surfaces have the boundary resistance of copper given by Eqs. (2a), (2b), and (3). In addition, it is assumed that no temperature gradients exist in a direction transverse to the flow in either stream or in the intermediate tube and that there is negligible conductivity in the tube walls parallel to the flow.

Calculations have been done for a heat exchanger 1 m long consisting of a 2 mm o.d. \times 0.1 mm wall and a 1 mm o.d. \times 0.1 mm wall tube, and a 1.5 m long exchanger of a 1.20 mm o.d. \times 0.076 mm wall and a 0.4 mm o.d. \times 0.076 mm wall tube. These sizes are typical of heat exchangers in current use. Conductivity effects in these exchangers are negligible at normal flow rates. However, it is of interest to compare the deviation predicted by Eq. (12) with the rigorous result found from a solution of Eq. (1) with and without conductivity terms. Only conductivity in the dilute liquid was considered, since including conductivity in both streams complicates the problem considerably and gives little additional information, as the concentrated stream conductance is usually much smaller. The value for κ_d used in Eq. (1) is given by

$$\kappa_d = (4.43T_d^{-0.96} + 4.87 \times 10^3 T_d^{0.81} - 2.2 \times 10^2) \left(\frac{\mu\text{W}}{\text{cm} \cdot \text{K}} \right), \quad (15)$$

where T is in degrees Kelvin. This expression approximately fits the data of Abel *et al.*^{13,14} interpolated to the proper concentration. This conductance in the dilute stream for the 1 m long exchanger raises the mixer temperature by 80 μK at $T_m = 16$ mK when the flow rate is 5×10^{-6} moles/sec. This is a deviation of 0.5%, and the value of 0.2% from the left side of Eq. (12) is in rough agreement. Increasing the cross sectional area of the dilute stream by a factor of 100 increases the actual deviation to 14% compared with 20% from Eq. (12).

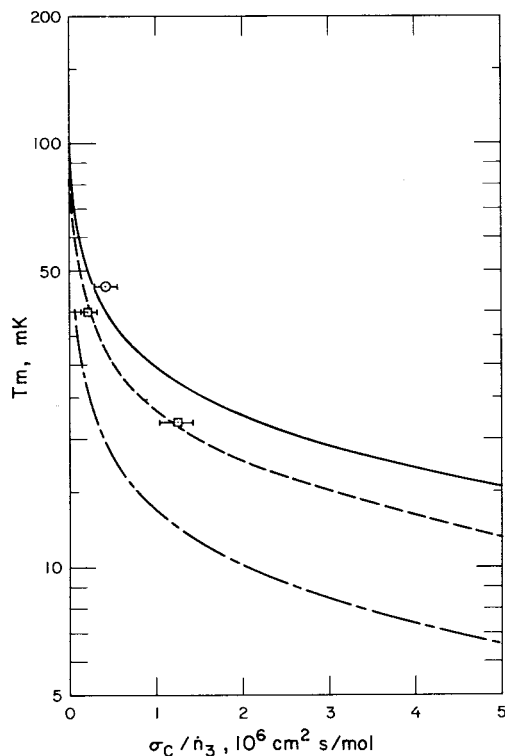


Fig. 7. Minimum mixer temperature T_m as a function of the concentrated stream surface area σ_c divided by ^3He flow rate \dot{n}_3 for an ideal continuous heat exchanger. The solid curve is for the Kapitza resistivities, ρ_c and ρ_d , the same as for copper. The dashed and broken curves are for both ρ_c and ρ_d reduced by the factors 1.8 and 20/3, respectively. The still temperature T_s is 0.7 K and $\sigma_d/\sigma_c = 1.6$. At the low temperature end, the curves behave nearly as $T_m \propto (\sigma_c/\dot{n}_3)^{-1/2}$. \circ —Anderson; \square —Wheatley.

In Fig. 7, the minimum mixer temperature, assuming zero heat leak, that can be reached using an ideal continuous heat exchanger, is shown as a function of the quantity σ_c/\dot{n}_3 , where σ_c is the total heat transfer surface in contact with the concentrated stream. The ratio σ_d/σ_c is 1.6, where σ_d is the total dilute side heat transfer surface, but there is little sensitivity to this ratio in the range 1–2 because ρ_c is the dominant resistivity. When the ratio is 2, T_m is about 1% less and for a ratio of 1, T_m is about 4% higher; thus, increasing only σ_d is of little value in trying to reduce T_m . The curve of T_j as a function of x is similar in shape to the curve of T_m as a function of σ/\dot{n}_3 .

Mixer temperatures obtained by Anderson^{8,19} and Wheatley²⁰ using coaxial tube exchangers are shown on Fig. 7. The error bars indicate uncertainty of \dot{n}_3 . Anderson's result for T_m is higher than the calculated curve. This could be due to a large heat leak, but more likely it is due to an actual temperature difference between the mixer and externally mounted CMN thermometer. Temperatures in Wheatley's refrigerator were measured inside the mixer and are lower than the calculated curve. Such behavior can be explained if ρ_c has a value which is one-half that used in this calculation. The value of ρ_d could also be reduced by a factor of 2 but the results for T_m are rather insensitive to

TABLE II. Change of calculated value of the mixer temperature T_m for the ideal continuous exchanger when various corrections are considered. The ΔT is the change of T_m from the value determined with no corrections included.

Type of correction	T_m (mK)	ΔT (mK)
No corrections	27.65	0
Conductivity in dilute stream	27.65	0.00
ρ_c is expressed as Eq. (2a) above 0.13 K	27.26	-0.39
C_e is for 95% solution instead of pure ^3He	28.08	+0.43
Still temperature is reduced to 0.5 K	27.60	-0.05

ρ_d . The dashed curve in Fig. 7 is for the case of both ρ_c and ρ_d reduced by a factor of 1.8 from the copper values. This curve is obtained simply by reducing σ_c/n_3 of the solid curve by a factor of 1.8. Reducing ρ_c by a factor of 2.1 and leaving ρ_d unchanged gives the same curve. The dashed curve fits Wheatley's measured results well, which suggests that Kapitza resistance to Cu-Ni is about a factor of 2 lower than it is for copper. Such a difference is not unreasonable when one considers the large variations in Kapitza resistance which have been reported.²¹ All other corrections or refinements to the calculated curve, which are discussed below, would either raise the calculated curve or have a negligible effect on it. Various corrections to the calculated curve have been determined for a heat exchanger made up of 1.0 and 2.0 mm o.d. by 0.1 mm wall tubing 1 m long. Calculated values of T_m for the various corrections are shown in Table II. The flow rate is 2×10^{-5} moles/sec and \dot{Q} is zero. Unless otherwise specified, the still temperature is 0.7 K, ρ_c is given by Eq. (2a), ρ_d by Eq. (3), the specific heats are the same as those discussed above, and $\kappa_j=0$.

In Table II, the first modification in the computation takes into account the reduction of the boundary resistance of the concentrated stream from $R \propto T^{-3}$ above 0.13 K. In the second modification, only C_e is changed. The calculated heat capacity of a 95% solution was used instead of the heat capacity of pure ^3He . These are the largest corrections but they essentially cancel each other. Heat conduction along the streams has no effect and a change in still temperature has very little effect. Other effects, such as heat leaks, viscous heating, and higher percentages of ^4He circulated, all raise T_m .

Anderson *et al.*¹² have estimated from experimental measurements that the boundary resistance between a plastic material (Epibond 100 A) and pure liquid ^3He is 3/20 of the value for copper. The broken line in Fig. 7 is for an exchanger in which both ρ_c and ρ_d are 3/20 of the copper values. A T_m of 10 mK could be obtained with a modest sized heat exchanger with plastic separating the streams if ρ_c and ρ_d are indeed this small for plastics. An Epibond 100 A member between the streams would need to be quite thin (the order of 0.1 mm) to prevent non-negligible temperature gradients across it. With large diameter plastic tubes, the heat exchanger could also serve as the mechanical support between the still and mixer.

Before a more detailed comparison can be made between the calculated and experimental performance of the coaxial heat exchangers, measurements are required of the Kapitza resistances of Cu-Ni and stainless steel tubes as well as more experimental data for T_m .

In many of the refrigerators presently in operation, the heat exchangers are either coaxial tube or discrete from the still to the mixer. Discrete exchangers are generally more efficient than the coaxial exchanger in terms of heat transferred per volume of liquid in the exchanger, even though they are less efficient in terms of heat transferred per unit surface area. Thus the discrete exchanger, with its high surface area per unit liquid volume, should always be used whenever practically possible. The calculations show, however, that only a 10 cm length of coaxial exchanger made of the 1 and 3 mm tubing discussed above is sufficient to cool the incoming ^3He from 0.7 to 0.2 K at a flow rate of 2×10^{-5} moles/sec. This length of exchanger has a σ_c of 2.4 cm^2 . A sintered copper powder heat exchanger with a surface area even as large as 6 cm^2 would only be a cube 2 mm on a side. The tubes connecting this tiny exchanger to the still and next exchanger can easily have the same volume that a coaxial exchanger would have. Hence, at least from $T_c=0.7$ to 0.2 K it is much more practical to

TABLE III. Enthalpies used in this work for ^3He in both the dilute and concentrated (pure ^3He) streams. The dilute and pure ^3He enthalpies are H_d and H_c , respectively. A constant must be added to H_d for $T_m > 0$.

T (K)	H_d (J/moles)	H_d/T^2 (J/moles · K ²)	H_c (J/moles)	H_c/T^2 (J/moles · K ²)
0.005	0.001340	53.62	0.000313	12.52
0.010	0.005373	53.73	0.001238	12.38
0.015	0.01213	53.92	0.002755	12.24
0.020	0.02167	54.18	0.004844	12.11
0.025	0.03407	54.51	0.007487	11.98
0.030	0.04941	54.90	0.01067	11.85
0.040	0.08932	55.82	0.01856	11.60
0.050	0.1422	56.88	0.02840	11.36
0.060	0.2086	57.95	0.04007	11.13
0.080	0.3820	59.69	0.06842	10.69
0.100	0.6056	60.56	0.1027	10.27
0.120	0.8725	60.59	0.1423	9.879
0.140	1.173	59.84	0.1862	9.499
0.160	1.498	58.52	0.2338	9.132
0.180	1.843	56.87	0.2844	8.777
0.200	2.202	55.04	0.3373	8.433
0.220	2.572	53.14	0.3922	8.103
0.240	2.951	51.23	0.4485	7.786
0.280	3.726	47.52	0.5643	7.198
0.320	4.516	44.11	0.6834	6.674
0.360	5.318	41.03	0.8053	6.214
0.400	6.127	38.29	0.9300	5.812
0.450	7.149	35.31	1.090	5.381
0.500	8.182	32.73	1.253	5.014
0.550			1.421	4.699
0.600			1.590	4.431
0.650			1.769	4.187
0.700			1.949	3.978
0.750			2.133	3.793
0.800			2.322	3.628
0.900			2.713	3.349
1.000			3.124	3.124

use a simple coaxial tube exchanger such as Ehnholm *et al.*⁴ have done.

The uncertainties of the specific heats of the liquids are as small as a few percent. The conductivities of the liquids are not known nearly so accurately, but in most cases the exact values of the conductivities are not critical. The conductances are so large in the low temperature discrete exchangers generally used that the exact value is unimportant since the liquid in the exchanger is nearly uniform in temperature. The dominating uncertainties in the calculations are the magnitudes of the Kapitza resistivities. There is only one measurement of the copper-dilute solution resistivity.³ There are two measurements of the copper-³He resistivity^{12,22} which essentially agree. Anderson²³ reports that the Kapitza resistivity is a factor of 4 lower for oxidized copper surfaces than it is for surfaces heated in a hydrogen atmosphere. This report, plus the wide variation of ⁴He boundary resistivities²¹ reported in the literature, indicate that ρ_c and ρ_d could vary widely. However, at present it is not known to what extent the Kapitza resistivities of actual heat exchanger surfaces might vary from those used in these calculations.

More calculations are in progress to determine the optimum sizes for discrete exchangers operating at low temperatures.

ACKNOWLEDGMENT

The authors wish to thank David E. Daney for many helpful discussions.

APPENDIX

The analytic expressions used in this work for the ³He specific heat, C_d , in the dilute side of the heat exchangers are

$$C_d = 107.16T + 6.1 \times 10^3 T^3 - 3.595619965 \times 10^5 T^5 \\ - 1.007454504 \times 10^8 T^7 + 1.755839768 \times 10^{10} T^9 \\ - 1.06390240 \times 10^{12} T^{11} + 2.273119224 \\ \times 10^{13} T^{13} \text{ J/moles} \cdot \text{K}, \quad (T \leq 0.12 \text{ K});$$

and

$$C_d = -6.250523127 + 300.6200772T - 1.467577784 \\ \times 10^3 T^2 + 3.842834281 \times 10^3 T^3 - 5.571748599 \\ \times 10^3 T^4 + 4.2081268534 \times 10^3 T^5 - 1.281475180 \\ \times 10^3 T^6 \text{ J/moles} \cdot \text{K}, \quad (0.12 < T \leq 0.5 \text{ K}).$$

The above expressions are valid for a mixer temperature of 0 K, but for a mixer temperature of 20 mK the maximum error is still less than 2%. The enthalpy of the dilute stream for $T_m=0$ is given by

$$H_d = \int_0^T C_d dT. \quad (\text{A1})$$

The enthalpy H_c of the concentrated stream is just that of pure ³He as tabulated previously by Radebaugh.¹⁵ Values of H_d , H_d/T^2 , H_c , and H_c/T^2 for several temperatures should be useful in heat exchanger calculations and are listed in Table III. All the enthalpies are for 1 mole of ³He in solution. For $T_m > 0$, the integration in Eq. (A1) is from T_m to T , and a constant equal to the enthalpy on the solubility curve¹⁵ must be added.

¹ H. E. Hall, P. J. Ford, and K. Thompson, *Cryogenics* **6**, 80 (1966).

² B. S. Neganov, N. Borisov, D. M. Liburg, *Zh. Eksp. Teor. Fiz.* **50**, 1445 (1966) [*Sov. Phys. JETP* **23**, 959 (1966)].

³ J. C. Wheatley, O. E. Vilches, and W. R. Abel, *Physics* **4**, 1 (1968).

⁴ G. J. Ehnholm, T. E. Katila, O. V. Lounasmaa, and P. Reivari, *Cryogenics* **8**, 136 (1968).

⁵ D. S. Betts and R. Marshall, *Cryogenics* **9**, 460 (1969).

⁶ H. Sheinberg and W. A. Stevert, Los Alamos Sci. Lab. Rep. No. LA-4259-MS.

⁷ P. Roubeau and E. Varoquanx, *Cryogenics* **10**, 255 (1970).

⁸ A. C. Anderson, Proc. 1970 Ultralow Temp. Symp., Washington, NRL Rep. 7133; *Rev. Sci. Instrum.* **41**, 1446 (1970).

⁹ D. S. Betts, *Contemp. Phys.* **9**, 97 (1968).

¹⁰ B. S. Neganov, preprint, Joint Institute for Nuclear Research, Dubna USSR, (JINR-P13-4014) (1968) [English transl. BNL-TR 234].

¹¹ CO-OP Program, D2 UTEX RKAMSUB.

¹² A. C. Anderson, J. I. Connolly, and J. C. Wheatley, *Phys. Rev.* **135**, A910 (1964).

¹³ W. R. Abel, R. T. Johnson, and J. C. Wheatley, *Phys. Rev. Lett.* **18**, 737 (1967).

¹⁴ W. R. Abel and J. C. Wheatley, *Phys. Rev. Lett.* **21**, 1231 (1968).

¹⁵ R. Radebaugh, *Nat. Bur. Stand. Tech. Note No. 362* (1967).

¹⁶ R. Radebaugh and J. D. Siegwarth, *Int. Conf. Low Temperature Phys.* 12th Kyoto, 1970 (to be published).

¹⁷ P. Roubeau, D. LeFur, and E. J.-A. Varoquanz, Proc. Int. Cryog. Eng. Conf. 3rd Berlin, 1970, p. 315.

¹⁸ R. Radebaugh and J. D. Siegwarth, Proc. 1970 Ultralow Temp. Symp. Washington, NRL Rep. 7133.

¹⁹ A. C. Anderson, private communication.

²⁰ J. C. Wheatley, private communication.

²¹ N. S. Snyder, *Nat. Bur. Stand. Tech. Note No. 385* (1969); *Cryogenics* **10**, 89 (1970).

²² D. M. Lee and H. A. Fairbank, *Phys. Rev.* **116**, 1359 (1959).

²³ See the discussion following the paper: R. Radebaugh and J. D. Siegwarth, Proc. Int. Inst. Refrig. Comm. I Meeting Tokyo, 1970, p. 57.

Journal Title: Review of Scientific Instruments

Volume: 42

Issue:

Month/Year: 1971

Pages: 1111-1119

Article Author: Siegwarth, J.D. et al

Article Title: Analysis of Heat Exchangers for Dilution Refrigerators

Notes:

Location:

Call No.:

Item #:

Requestor:

Ray Radebaugh (radebaug)

Phone: 3710

838.09

WARNING CONCERNING COPYRIGHT RESTRICTIONS

The copyright law of the United States (Title 17, United States Code) governs the making of photocopies or other reproductions of copyrighted materials.

Under certain conditions specified in the law, libraries and archives are authorized to furnish a photocopy or other reproduction. One of these specified conditions is that the photocopy or reproduction is not to be "used for any purpose other than private study, scholarship, or research". If a user makes a request for, or later uses, a photocopy or reproduction for purposes in excess of "fair use", that user may be liable for copyright infringement.

Boulder Labs Library reserves the right to refuse to accept a copying order if, in its judgment, fulfillment of the order would involve violation of copyright law.